cognizancejournal.com
Rajab Ali Khavari *et al*, Cognizance Journal of Multidisciplinary Studies, Vol.4, Issue.4, Apr 2024, pg. 235-243
(An Open Accessible, Multidisciplinary, Fully Refereed and Peer Reviewed Journal)
ISSN: 0976-7797
Impact Factor: 4.843
Index Copernicus Value (ICV) = 77.57

Using Lithium-6 Filter for Study of Dose Distribution with Max. and Min. Displacement of Prostate Inside the Body by BNCT Method

Rajab Ali Khavari[1]; Dawod Mirzaee[2]

[1]Physics faculty, Kabul University, Afghanistan
[2]Physics faculty, Kabul University, Afghanistan
[1] Khavary81@gmail.com; [2] Dmirzaee@gmail.com

DOI: 10.47760/cognizance.2024.v04i04.016

Abstract- Physical dose assessment of prostate tumor and adjacent healthy tissues in ORNL, adult male (AM) and KTMAN-2 phantoms was performed using the Monte Carlo transport code. Two different spectra of MIT reactor (without and with lithium filter) were considered. To evaluate the effectiveness of this method in destroying cancer cells for different depths of the prostate, the prostates were moved three times with a distance of 3 cm towards the surface of the body. In addition, the effects of using a lithium filter with different thicknesses on the physical doses of the prostate and adjacent healthy tissues were investigated. It has been observed that decreasing the depth of the prostate increases the physical dose received by the tumor. When the prostate is placed at the maximum depth inside the body, the tissues located in the path of the beam receive the maximum amount of dose. However, the use of a lithium filter reduces damage to healthy tissues, so that when the prostate is near the surface of the body, the lithium filter increases the amount of dose delivered to tumors. In these conditions, the average energy of the penetration distance of epithermal neutrons and neutrons in tissues increases. By changing the location of the prostate gland inside the body, the physical doses of normal tissues did not change, but it was observed that increasing the thickness of the lithium filter significantly reduced the dose of normal tissues.
Keywords- MIT neutron spectrum, BNCT, Prostate tumor, Lithium-6 filter, Voxel phantoms

I. Introduction

BNCT simulations require thorough understanding of radiation and nuclear interaction of neutrons with boron-10 and comprehensive knowledge of computational phantoms used in radiotherapy. In the interaction of thermal neutrons with boron-10, alpha and lithium particles are produced with energies of 1.4 and 0.8MeV, respectively, so that their ranges in water are about micrometer [1], [2] . Therefore, in treatment with BNCT low-range properties, RBE and high LET as well as the fragility feature of two or multiple alpha and lithium particles are used [2] . In the treatment of prostate cancer, the most important tissues receive large doses such as bladder, testis, skin and soft-tissues located behind the tumor, and in some phantoms such as KTMAN-2, the pelvis of bone tissue is also present. Table I shows the constituent elements of these tissues with respect to the reference data of ICRU 46 [3]. Neutron interactions of tissues contain high amounts of hydrogen and nitrogen, are usually nitrogen capture (proton recoil) and hydrogen capture (photon dose), so significant undesirable doses are delivered to these tissues [4], [5]. Since

cognizancejournal.com
Rajab Ali Khavari *et al*, Cognizance Journal of Multidisciplinary Studies, Vol.4, Issue.4, Apr 2024, pg. 235-243
(An Open Accessible, Multidisciplinary, Fully Refereed and Peer Reviewed Journal)
ISSN: 0976-7797
Impact Factor: 4.843
Index Copernicus Value (ICV) = 77.57

the prostate positions were different in each of the phantoms, epithermal neutron spectrum of MIT reactor (with and without the lithium-6 filter) was considered as neutron source. It should be mentioned that, the boron concentration in the tumor is several times more than those of the nearby healthy tissues.

II. Materials & Methods

A-Monte Carlo Calculations

MCNP computational code is an important tool to simulate epithermal neutron spectrum and flux in the BNCT method [6]. To evaluate dose due to the transported particles in the various organs, mesh tally, lattice tally (depth dose estimations) and + F6 tally (total dose estimations) were used [7].

B-Phantom Implementation

In this research, the dose distribution in a prostate tumor was studied in three phantoms. The organ doses were calculated in ICRP reference adult male, KTMAN-2 voxel and M1RD-ORNL phantoms. Supplementary data file provided by ICRP represents 3D matrix of' 254 × 127 × 222 dimension with voxel resolution of 2.137 × 2.137 × 8 mm^3 for adult male (AM). The organ masses and body dimension were matched to the reference values reported by ICRP Publication 89 [8]. The densities and elemental compositions for organs and tissues provided in ICRP Publication 110 [9], were used in the Monte Carlo simulations.

KTMAN-2 is a Korean typical voxel phantom represents a 3D matrix with dimension and voxel resolution of 300 × 150 × 344 and 2×2 ×5 mm^3, respectively. Composition and densities of organs were readjusted with reference values reported by ICRP 89 and ICRI5 46 [3], [8]. Phantom MIRD-ORNL is an adult male mathematical phantom in which prostate gland is defined as the sphere with radius of 2.2 cm. Organs densities and body dimensions in a mathematical phantom were adjusted with reference values reported by ICRLT 46 implementation. To evaluate the effect of prostate depth in dose received by the tumor and its nearby tissues, the pelvis area of voxel phantoms were examined and depths of prostates relative to body surface were calculated for these phantoms. The maximum emplacement was 3 cm.

If the origin of coordinates of AM voxel phantom is considered at the right corner, the center of mass of its prostate gland would be at x=26.33, y=15.58 and z=90.07 cm. The distance between prostate and skin of AM is 8.5 cm. By moving prostate once with an interval of 3 cm in the opposite direction of y-axis toward the body surface (Δy =3 cm), the depth location of prostate varies between 5.5 cm (Δy =3 cm) and 8.5 cm (Δy=0 cm). The center of mass of a prostate gland of KTMAN-2 relative to the center of phantom is at x=-2, y=1 and z=-3.5 cm. The distance between prostate and skin of KTMAN-2 is 7.5 cm. As before, the prostate of KTMAN-2 was moved with an interval of 3 cm in the opposite direction of y-axis toward the body surface. Moreover, the center of mass of prostate gland of MIRD-ORNL, relative to its center, is at x=0, z=3 cm. Considering that the pelvis of voxel phantoms was located in front of the prostate gland, voxel phantoms were rotated around the x-axis (relative to the center of mass) in order that pelvis was not located between prostate and source any more. The degree of rotation around the x-axis for two voxel phantoms was different and small (approximately 8^o). From figure 1, it seems that this small rotation is reasonable and does not cause great variations in

cognizancejournal.com
Rajab Ali Khavari *et al*, Cognizance Journal of Multidisciplinary Studies, Vol.4, Issue.4, Apr 2024, pg. 235-243
(An Open Accessible, Multidisciplinary, Fully Refereed and Peer Reviewed Journal)
ISSN: 0976-7797
Impact Factor: 4.843
Index Copernicus Value (ICV) = 77.57

voxel phantoms anatomy. The prostate displacement along y-axis toward the body surface is shown in figure 1.

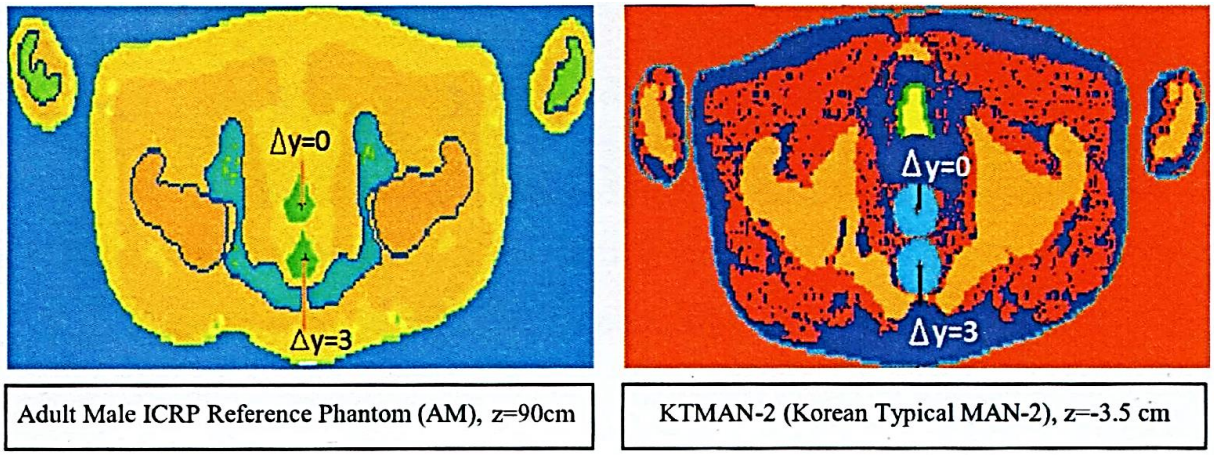

Figure 1. Prostate displacement relative to the body surface, Δy=0 to Δy=3, for he voxel phantoms (AM and KTMAN-2)

C- Boron Concentrations in Prostate Cancer

Maximum amount of dose delivered in BNCT method is resulted from neutron capture of boron-10. Thus, the distribution of boron in prostate tissue would be very important. On the other hand, boron-10 carrier drugs accumulate not only in cancer cells but also in nearby healthy tissues [10] [11] , [12], [13] So, if boron concentrations in tumors were low (relative to healthy tissues) undesirable doses would be delivered to healthy tissues (table 1).

Table 1. Constituent elements and density of the prostate gland and its adjacent tissues in percent.

Row	Type of tissue	Density ($gr.cm^3$)	H	C	N	O	Ca	Na	P	S	Cl	K
1	Bone	1.4	7.3	25.5	3.1	47.9	10.2	0.3	5.1	0.2	0.1	0.1
2	Soft Tissue	1.03	10.5	25.6	2.7	60.2	-----	0.1	0.2	0.3	0.2	0.2
3	Skin	1.09	10.0	20.4	4.2	64.5	-----	0.2	0.1	0.2	0.3	0.1
4	Prostate	1.03	10.5	25.6	2.7	60.2	-----	0.1	0.2	0.3	0.2	0.2
5	Testes	1.04	10.6	9.9	2.0	76.6	-----	0.2	0.1	0.2	0.2	0.2
6	Bladder	1.04	10.5	9.6	2.6	76.1	-----	0.2	0.2	0.2	0.3	0.3

D- Epithermal Neutron Source

Three basic parameters are very influential in choosing neutron sources used in BNCT: energy, intensity, and pollution. In BNCT, a neutron flux of 10^9 $n.cm^{-2}s^{-1}$ is often required to prevent increasing the undesired dose in the healthy tissues surrounding the prostate gland [14]. In this study, the epithermal neutron beam from MIT research reactor was the primary neutron source for calculation of the depth dose distributions in prostate cancer, which has an epithermal flux of 3.71×10^9 $n.cm^{-2}.s^{-1}$(table 2) [15] .

cognizancejournal.com
Rajab Ali Khavari *et al*, Cognizance Journal of Multidisciplinary Studies, Vol.4, Issue.4, Apr 2024, pg. 235-243
(An Open Accessible, Multidisciplinary, Fully Refereed and Peer Reviewed Journal)
ISSN: 0976-7797
Impact Factor: 4.843
Index Copernicus Value (ICV) = 77.57

Table 2. Beam parameters for active reactor in the BNCT.

Characteristics parameters of the MIT reactor epithermal neutron spectrum for BNCT method					
Reactor	Country	Power (MW)	ϕ_{epi} 10^{9}[n/cm^2-s]	D_{fast}/ϕ_{epi} 10^{-13}[Gy-cm^2/n]	D_{gama}/ϕ_{epi} 10^{-13}[Gy-cm^2/n]
MIT	USA	5	3.71	1	3.6

It was reported that when tumors are seated deep inside the body, it would be better to tailor neutron spectrum by using an 8 mm lithium filter to remove the low energy parts of the spectrum, which just increase the radiation dose in healthy tissue placed in neutron beam path [16]. In figure 2, the neutron flux of MIT reactor with and without lithium filter is displayed. 55% reduction in neutron flux is obtained using lithium filter.

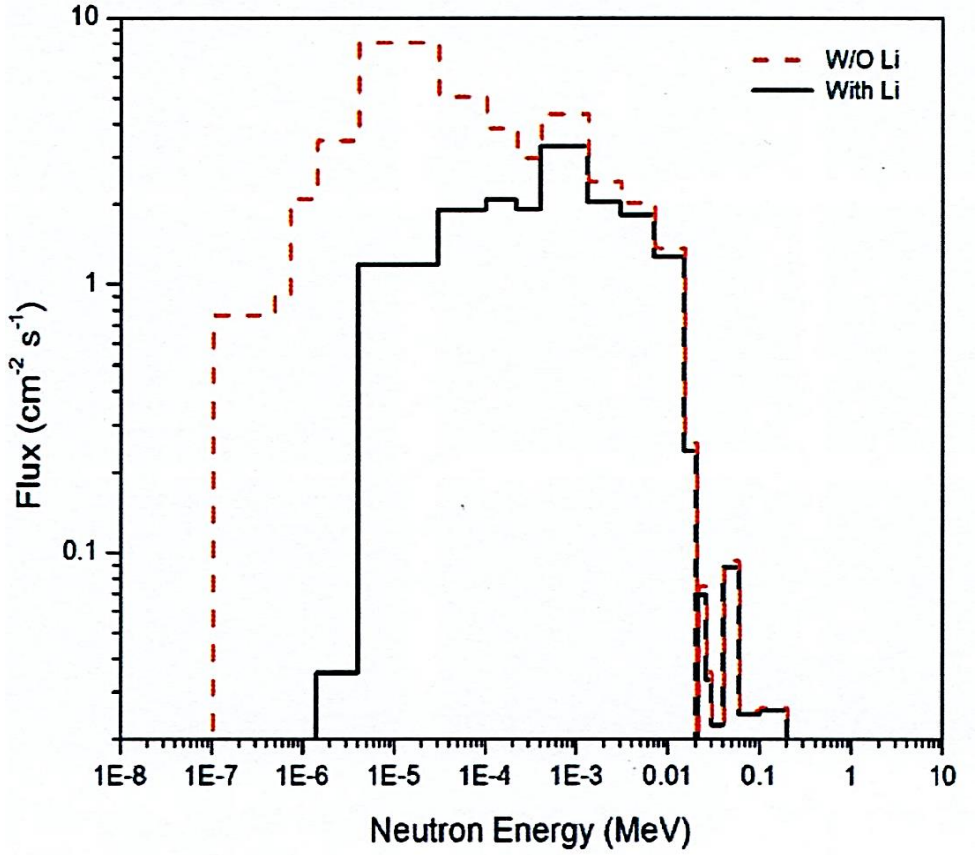

Figure 2. MIT neutron flux without (red dashed-line) and with (black line) lithium filter.

E- Lithium-6 Filter

High energy epithermal neutrons have high penetration depths inside patient body (about 10 cm) and the dominant process that they lose their energies by is elastic scattering. Thus, in this study the spectrum of high energy epithermal neutrons has been used. In order to reduce the amount of absorbed dose in the normal organs before the tumor, the lithium filter applied to remove the low energy neutrons from the incident spectrum. It can be seen that the mean penetration depths of the epithermal neutrons without and with

cognizancejournal.com
Rajab Ali Khavari *et al*, Cognizance Journal of Multidisciplinary Studies, Vol.4, Issue.4, Apr 2024, pg. 235-243
(An Open Accessible, Multidisciplinary, Fully Refereed and Peer Reviewed Journal)
ISSN: 0976-7797
Impact Factor: 4.843
Index Copernicus Value (ICV) = 77.57

lithium filter are 9.3 cm and 9.9 cm, respectively. In this investigation, the lithum-6 filter with length of 8 mm has been used [16].

The neutron flux after passing the filters is different for various lithium-6 filter thicknesses. As the thickness of the lithium-6 filter increases, neutron flux decreases. In order to select the appropriate filter, the effect of 6 mm to 10 mm lithium filter was investigated (Table 3) [16]. Table 3 shows that the neutron flux in the body phantom using different thicknesses of lithium-6 filter decreases. In the present study, since thermal and fast neutrons fluxes are very small, considering them in simulations do not affect the distribution of depth-dose.

Table 3. Neutron flux (cm^{-2}.s-) in air for Lithium-6 filter with different thicknesses.

Neutron flux($cm^{-2}s^{-1}$) in air at the surface (with Lithium filter of different thickness)						
Energy	0-0.5eV			0.5-10 eV		
Condition	flux	error	ratio	flux	error	ratio
No filter	5.52E+7	0.025	100%	3.01E+9	0.009	100%
6mm lithium	3.14E+6	0.077	5.7%	1.67E+9	0.014	55.5%
8mm Lithium	2.21E+6	0.104	4.0%	1.52E+9	0.014	50.5%
10mm Lithium	1.85E+6	0.088	3.4%	1.36E+9	0.015	45.2%
Energy	10-20keV			total		
Condition	flux	error	ratio	flux	error	ratio
No filter	1.15E+8	0.034	100%	3.18E+9	0.009	100%
6mm lithium	9.60E+7	0.041	83.5%	1.76E+9	0.013	55.3%
8mm Lithium	9.41E+7	0.041	81.8%	1.61E+9	0.014	50.6%
10mm Lithium	9.79E+7	0.040	85.1%	1.46E+9	0.014	45.9%

F- Dose Estimation

Boron concentration in the tumor should be high enough (about three to six times higher than the nearby healthy tissues) [17]. Thus, the boron concentration of 30 ppm and 5 ppm were considered in the prostate gland and nearby healthy tissues, respectively [10] [11] , [12], [13]. In this study, regardless of RBE values, physical dose was calculated by MCNP code. In order to evaluate the uniformity of the dose distribution, the maximum and minimum tumor dose was examined. In addition, to compare the physical dose of healthy tissue and tumor, the coefficient of variation (CV) and the ratio of average dose of tumor to the maximum dose delivered to healthy tissue (TNR) were investigated. For a more detailed study, the mesh tally type three has also been used for dose distribution.

III. Results and Discussions

Maximum physical dose received by healthy tissue near the prostate are presented in Table 4 for two different neutron spectra (with and without the lithium-6 filter). By changing the position of the prostate gland, the physical doses of healthy tissues around the tumor do not change and the obtained values are valid for all tumor depths.

cognizancejournal.com
Rajab Ali Khavari *et al*, Cognizance Journal of Multidisciplinary Studies, Vol.4, Issue.4, Apr 2024, pg. 235-243
(An Open Accessible, Multidisciplinary, Fully Refereed and Peer Reviewed Journal)
ISSN: 0976-7797
Impact Factor: 4.843
Index Copernicus Value (ICV) = 77.57

Table 4. Physical dose in Gy.min^{-1} for soft tissue, urinary bladder, rectum and skin with two neutron spectra of MIT reactor (without and with lithium filter) for AM phantom.

Maximum physical dose(Gr/min)					
Li filter		Soft tissue	Bladder wall	Rectum wall	skin
AM phantom	Without	0.20	0.10	0.02	0.15
	with	0.07	0.04	0.01	0.07
KTMAN-2 phantom	Without	0.07	0.08	0.07	0.08
	with	0.04	0.06	0.03	0.03
MIRD-ORNL phantom	Without	0.09	0.14	0.06	0.07
	with	0.04	0.06	0.05	0.02

The maximum, minimum and average amounts of physical dose received by tumor together with CV and TNR. with and without lithium filter were specified at different depths of a prostate gland (for three phantoms) in table 5. The numbers in the table have been rounded to two decimal places. Given the results, decreasing the distance between prostate and body surface increases the maximum, minimum and average values of physical dose in tumor. Considering the uniformity of dose, smallest values of CV at Ay=3 cause more uniformity in treatment region. Figure 3 illustrates the dose distribution at z=-3.5 (Korean Typical MAN-2 voxel phantom) for different distances of tumors from the body surface for two MIT fluxes (with and without lithium filter). Because dose values differ in each situation, the isodose curves were normalized to their maximum amount. It is observed from figure 3 that by decreasing the distance from the body surface, the physical dose of prostate increases, while the contribution of healthy tissues in receiving the dose decreases.

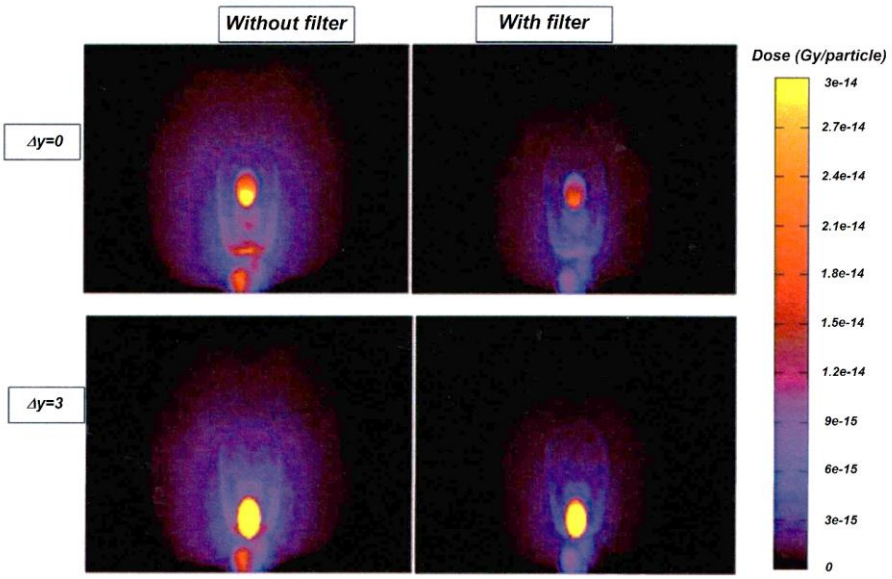

Figure 3. Dose distribution at r=-3.5 for neutron spectrum of MIT reactor without and with lithium filter at Δy-0 and Δy=3 (KTMAN-2 phantom).

cognizancejournal.com
Rajab Ali Khavari *et al*, Cognizance Journal of Multidisciplinary Studies, Vol.4, Issue.4, Apr 2024, pg. 235-243
(An Open Accessible, Multidisciplinary, Fully Refereed and Peer Reviewed Journal)
ISSN: 0976-7797
Impact Factor: 4.843
Index Copernicus Value (ICV) = 77.57

Table 5. Maximum, minimum, and average physical dose of tumor together with V and TNR at different depth Locations of prostate for two MIT spectra.

		Without filter		With filter	
phantom	Tumor dose	0 cm	3 cm	0 cm	3 cm
AM(ICRP Re.)	Max(Gy/min)	0.11	0.32	0.05	0.13
	Min(Gy/min)	0.003	0.11	0.01	0.05
	Ave(Gy/min)	0.07	0.22	0.03	0.09
	CV(%)	26	23	24	20
	TNR	0.33	1.08	0.44	1.28
KTMAN-2	Max(Gy/min)	0.16	0.36	0.08	0.20
	Min(Gy/min)	0.04	0.13	0.01	0.06
	Ave(Gy/min)	0.09	0.25	0.05	0.13
	CV(%)	12	10	13	11
	TNR	0.80	1.80	0.02	1.00
MIRD-ORNL	Max(Gy/min)	0.17	0.45	0.06	0.09
	Min(Gy/min)	0.04	0.12	0.01	0.03
	Ave(Gy/min)	0.10	0.29	0.04	0.06
	CV(%)	10	9	15	10
	TNR	0.62	1.68	0.35	0.60

The effect of different thicknesses of lithium-6 filter on the dose distribution was examined in three phantoms for a known concentration and distance between the prostate and body surface. The results are shown in Figure 4. According to this figure, the higher thicknesses of the lithium-6 filter, decrease undesirable dose in healthy tissues resulted from the low-energy neutron. However, maximum thickness of lithium-6 filter cannot be used for deep tumors, because, although it reduces the damages to healthy tissues located around the tumor, it also decreases the dose received by the tumor.

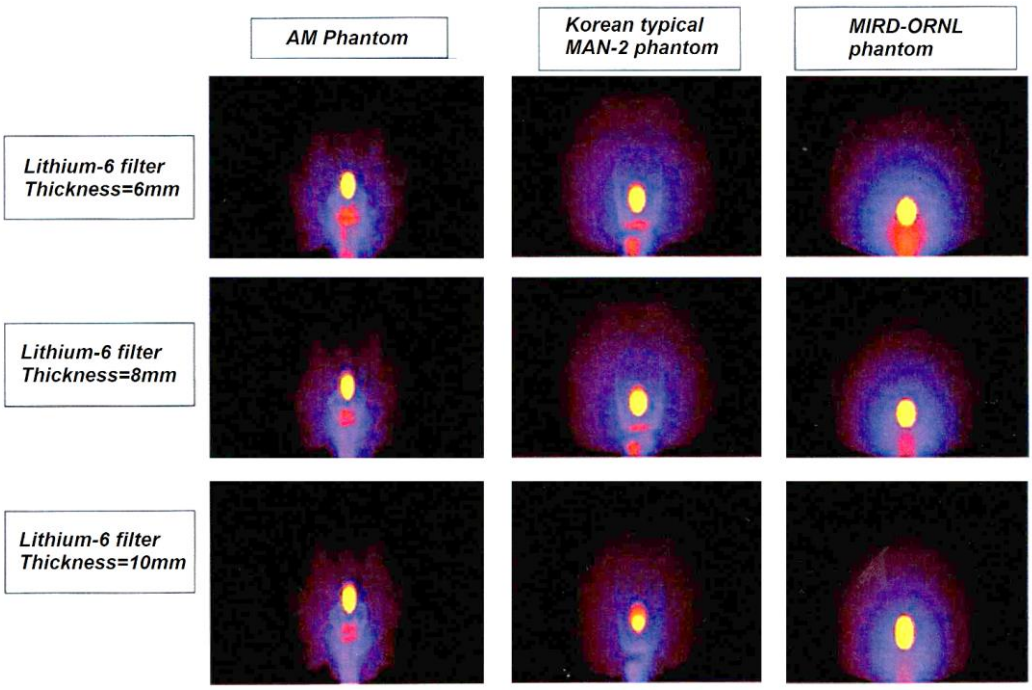

Figure 4. Dose distributions for three phantoms with different thicknesses of lithium-6 filter (6, 8 and 10 nm)

ISSN: 0976-7797
Impact Factor: 4.843
Index Copernicus Value (ICV) = 77.57

IV. Conclusion

Considering the obtained results, in all the healthy tissues, the physical dose due to MIT neutron spectrum with lithium-6 filter is smaller than that of MIT spectrum without the lithium-6 filter. By decreasing the total neutron flux using the lithium-6 filter the physical doses of healthy tissues decreased. Doses received by healthy tissues, which are near the prostate, are more than farther healthy tissues, but since the physical dose due to neutron flux without lithium filter is less than that with lithium filter, and their values are small, it is negligible. Thus, when the prostate is close to the body surface, the dose distribution is more uniform in the treatment area and physical dose absorbed in the tumor is much more than nearby healthy tissues. This process has been observed for both spectra (with and without the lithitun-6 filter), but results are more acceptable for the MIT neutron flux with lithium filter. This is due to the fact a part of thermal neutron spectrum will be removed and absorbed by lithium filter, and smaller amounts of dose are delivered to tissues located in the beam path, so that damages to healthy tissues decreased.

Depth dose assessment for prostate cancer treatment using the epithermal neutron beam of MIT reactor for MIRD-ORNL, ICRP (AM) and KTMAN-2 showed that in the presence of Lithium filter and for equal distance between the prostate and body surface, average mean physical dose does not very significantly. There are some important factors, which should be considered in BNCT method to avoid creating, undesirable dose in normal tissues; such as 1) selecting appropriate ratio of boron-10 concentration in the prostate gland and nearby healthy tissues, 2) determining the optimum distance between the prostate tumor and neutron source. We evaluate this distance in the range of 2 to 5 cm to have a good performance. Moreover, there is a need to choose the proper lithium filter with sufficient thickness to avoid undesirable dose in tumor and healthy tissues.

Acknowledgement

This article has been written with the cooperation of the dear professors of the Department of Physics, Faculty of Science, Ferdowsi University of Mashhad, especially Dr. Miri Hakimabad and Dr. Motavalli, for which we are grateful.

References

---

[1] M. D. Mizaee, S. H. Miri-Hakimabad and L. R. Motavalli, "Depth dose evaluation for prostate cancer treatment using boron neutron capture therapy," *Journal of Radioanalytical and Nuclear Chemistry*, vol. 302, no. 3, pp. 1095-1101, 2014.

[2] F. S. Rasuoli and S. F. Masoudi, "Simulation of the BNCT of Brain Tumors Using MCNP Code: Beam Designing and Dose Evaluation.," *Iranian Journal of Medical Physics*, vol. 9, no. 3, pp. 183-192, 2012.

[3] J. A. Scott, "Photon, Electron, Proton and Neutron Interaction Data for Body Tissues ICRU Report 46," *Journal of Nuclear Medicine January*, vol. 34, no. 1, 1992.

[4] T. Matsumoto, "Monte Carlo simulation of depth–dose distribution in several organic models for boron neutron capture therapy," *nuclear-instruments-and-methods-in-physics-research*, vol. 580, no. 1, pp. 552-557, 2007.

[5] M. E. El-Zaria, A. R. Genady, N. Janzen, C. A. Petlura, D. R. Beckford Vera and J. F. Valliant, "Preparation and evaluation of carborane-derived inhibitors of prostate specific membrane antigen (PSMA)," *Dalton Trans.*, vol. 43, no. 13, pp. 6-12, 2014.

[6] S. M. Sze and K. K. Ng, Physics of semiconductor devices, 3 ed., Wiley&Son, 2007.

[7] D. B. Pelowitz, *MCNP X2.6.0, LANL, LA-CP-07-1473*, 2008.

[8] J. Valentin, "Basic anatomical and physiological data for use in radiological protection,ICRP Publication 89," *Annals of the ICRP/ICRP Publication*, vol. 32, no. 3-4, pp. 1-227, 2003.

[9] M. Zankl, "Adult Male and Female Reference Computational Phantoms (ICRP Publication 110)," *Jpn. J. Health Phys*, vol. 45, no. 4, pp. 357-69, 2010.

[10] H. Joensuu, L. Kankaanranta, I. Auterinen, M. Kallio, M. Kulvik and J. Laakso, "Boron neutron capture therapy of brain tumors: clinical trials at the Finnish facility using boronophenylalanine," *Journal of Neuro-Oncology*, vol. 62, pp. 123-34, 2003.

[11] M. Viaggi, M. Dagrosa, J. Longhino, H. Blaumann, O. Calzetta, S. Kahl, G. Juvenal and M. Pisarev, "Boron neutron capture therapy for undifferentiated thyroid carcinoma: preliminary results with the combined use of BPA and BOPP," *Applied Radiation and Isotopes*, vol. 61, no. 5, pp. 905-0, 2004.

[12] T. Blue and J. Yanch, "Accelerator-based epithermal neutron sources for boron neutron capture therapy of brain tumors.," *Journal of Neuro-Oncology*, vol. 62, pp. 19-31, 2003.

[13] V. Nievaart, Spectral tailoring for boron neutron capture therapy, IOS press, 2007.

[14] F. Attix, Introduction to radiological physics and radiation dosimetry, New york: Wiley-VCH, 2004.

[15] K. Nakai, T. Yamamoto, H. Kumada and A. Matsumura, "Boron Neutron Capture Therapy for Glioblastoma: A Phase-I/II Clinical Trial at JRR-4," *European Association of NeuroOncology Magazine*, vol. 4, no. 3, pp. 116-23, 2014.

[16] W. Goa, Lithium-6 filter for a fission converter-based boron neutron capture therapy irradiation facility beam: Graduate Theses, Massachusetts Institute of Technology, 2005.

[17] F. Wagner, B. Loeper-Kabasakal and H. Breitkreutz, "Neutron medical treatment of tumors a survey of facilities," *Journal of Instrumentation*, vol. 7, pp. 1-10, 2012.

